RSC Advances

PAPER

View Article Online
View Journal | View Issue

Cite this: *RSC Adv.*, 2023, **13**, 26366

Surface-modified magnetite nanoparticles using polyethylene terephthalate waste derivatives for oil spill remediation

Mahmood M. S. Abdullah, * Hamad A. Al-Lohedan and Noorah A. Faqihi

This work aims at synthesizing new cross-linked poly ionic liquids, CPILs, VIMDE-Cl and CPIL, VIMDE-TFA, utilizing polyethylene terephthalate waste as a precursor and applying them to magnetite nanoparticles surface modification, producing surface-modified magnetite nanoparticles, SMNPs, VDCL/MNPs, and VDTA/MNPs, respectively. The structures of VIMDE-Cl and VIMDE-TFA, VDCL/MNPs, and VDTA/MNPs, were verified using different techniques. The particle sizes of SMNPs, VDCL/MNPs, and VDTA/MNPs, were evaluated with a transmission electron microscope and dynamic light scattering. The compatibility of VDCL/MNPs and VDTA/MNPs with crude oil components and their response to an external magnet were also measured using contact angle measurements and a vibrating sample magnetometer. The data confirmed the formation of SMNPs, nanosized structure, compatibility with oil components, and response to an external magnet. For that, VDCL/MNPs and VDTA/MNPs were applied for oil spill recovery using different SMNP : crude oil weight ratios. The impact of contact time on SMNPs' performance was also evaluated. The data indicated increased performance with an increase in SMNPs ratio, reaching maximum values of 99% and 96% for VDCL/MNPs and VDTA/MNPs, respectively, at SMNPs : crude oil ratio of 1 : 1. According to the results, the optimal contact time was 6 min, resulting in 89% and 97% performance for VDCL/MNPs and VDTA/MNPs at 1 : 4 SMNPs : crude oil ratio.

Received 4th July 2023
Accepted 24th August 2023

DOI: 10.1039/d3ra04457b

rsc.li/rsc-advances

1 Introduction

Polyethylene terephthalate (PET) is one of the most widely manufactured plastics in the world. It is estimated that the number of PET bottles used every minute is about one million worldwide.[1] In addition, PET has many other applications, including textiles, electrical insulation polymers, and other household materials. Using PET in these various applications produces vast amounts of solid waste. As environmental regulations have become more demanding in the last few decades, recycling or reusing these wastes has become increasingly critical. The use of these solid wastes to yield beneficial materials would have a dramatically positive effect on reducing solid waste. PET was reused to produce materials for different applications, including oil spill absorbers,[2] oil spill dispersants,[3] corrosion inhibitors,[4,5] azo dyestuff,[6] and electrochemical sensors.[7,8] Different PET-based amphiphilic compounds were prepared and employed in our earlier works to demulsify heavy crude oil emulsions.[9–11]

Oil spills in the seas and oceans are among the most significant sources of marine water contamination. Oil spills in marine environments can cause severe impacts on these environments. The amount of crude oil spilled in marine environments in 2017 was estimated at 7000 tons.[12] When crude oil covers water bodies, it can compromise light transmission through water and gas transfer between water and air, affecting aquatic life.[13,14] Several techniques are available for oil spill recovery, including physical (skimmers and booms), chemical (adsorbents and dispersants), and bioremediation.[15] Since these techniques do not provide comprehensive results for separating oil from water, nanotechnology is increasingly used to remove oil spills from marine water.[16] In recent years, using nanoparticles in oil spill recovery has attracted more attention due to their unique features, including high surface area, eco-friendly, high adsorption capacity, and reusability. Several nanoparticles were employed, such as magnetite (Fe_3O_4) carbon nanotubes, graphite, graphene, and titanium dioxide (TO_2). Due to their exceptional magnetic properties and high oil removal performance, magnetite nanoparticles (MNPs) are one of the most commonly applied nanoparticles for oil spill recovery.[17] After oil adsorption on MNPs' surfaces, they can be collected easily by an external magnetic field. Our previous works employed surface-modified magnetite nanoparticles (SMNPs) with plant extracts, ionic liquids, and amphiphilic compounds for oil spill recovery. In this study, PET waste was used for preparing two novel cross-linked poly ionic liquids (CPIL), where the letters were used to modify the surface of MNPs. SMNPs were used for oil spill recovery.

Department of Chemistry, College of Science, King Saud University, P.O. Box 2455, Riyadh 11451, Saudi Arabia. E-mail: maltaiar@ksu.edu.sa

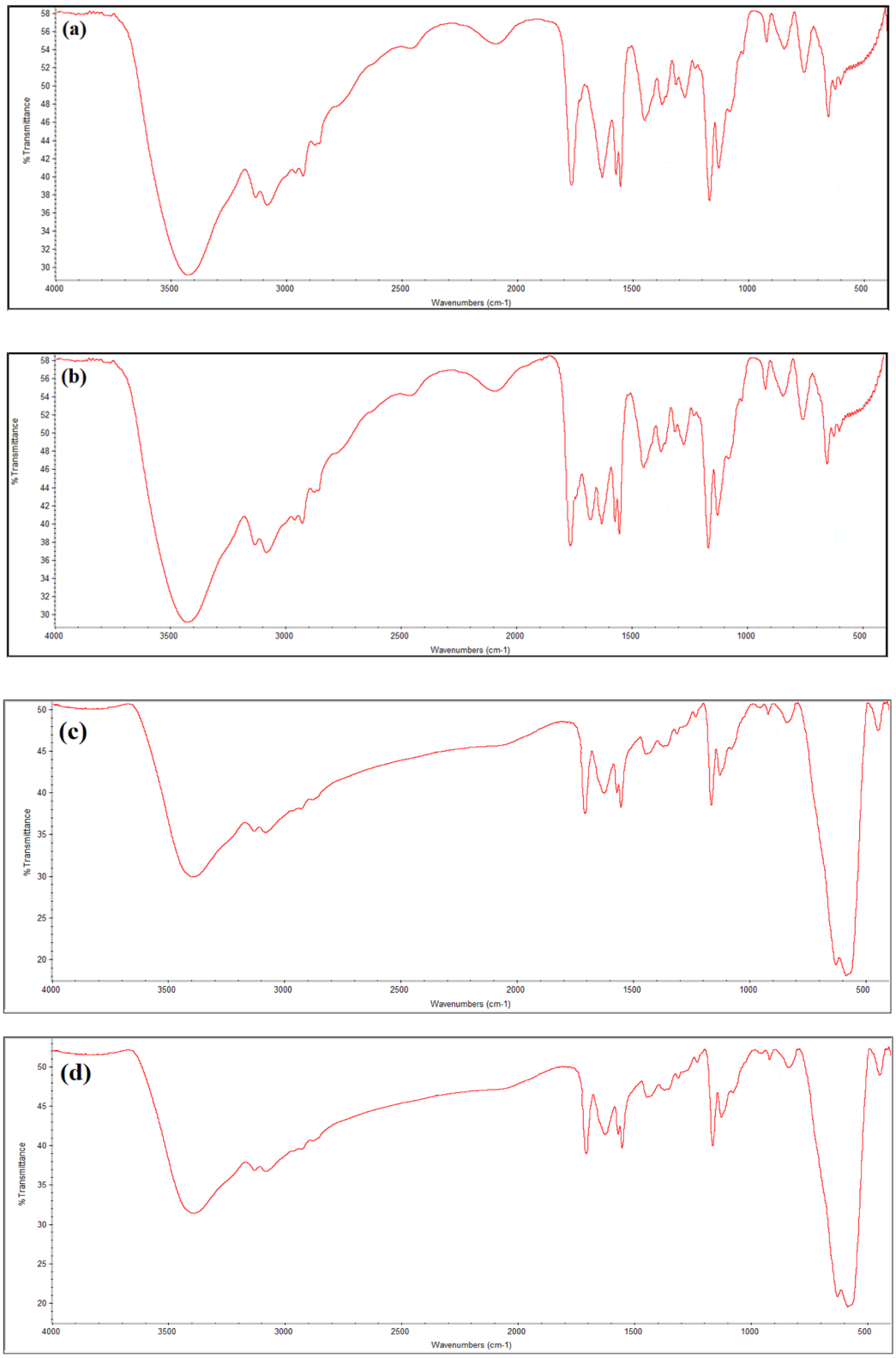

Fig. 1 FTIR spectra of (a) VIMDE-Cl, (b) VIMDE-TFA, (c) VDCL/MNP, and (d) VDTA/MNPs.

2 Experimental

2.1. Materials

PET waste was used for preparing bis(2-hydroxyethyl) terephthalate (BHET), which was converted to the alkyl halide, bis(2-chloroethyl)terephthalate (BCET), as reported earlier.[11] 1-Vinylimidazole (VIM), 2,2′-dichlorodiethyl ether (DE), dimethylformamide (DMF), hydrated ferric chloride ($FeCl_3 \cdot 6H_2O$) ferrous chloride ($FeCl_2 \cdot 4H_2O$), and ammonium hydroxide solution were obtained from Sigma-Aldrich Co. Crude oil was supplied by Al-Riyadh refinery unit, ARAMCO Co., Riyadh, Saudi Arabia. Its full chemical and physical properties were reported in our earlier work.[18]

VIM (10 g, 106 mmol) was diluted with 15 mL of DMF and stirred at 25 °C for 15 minutes in a three-neck-bottom flask supplied with a thermometer and nitrogen inlets. The temperature was increased to 65 °C overnight while the mixture was continually stirred, after adding AIBN (0.005 wt% related to VIM monomer). After that, a mixture of cross-linker reagents, DE (3.8 g, 26.5 mmol) and BCET (7.7 g, 26.5 mmol), was dissolved in DMF (35 mL) and added slowly to the obtained polymer solution (poly (vinylimidazole)). After 72 hours of stirring and heating at 70 °C, CPIL, VIMDE-Cl was washed with DMF, then water, and kept at 60 °C in an oven to evaporate solvents, getting a constant weight. For preparing the second CPIL, VIMDE-TFA, 4 g of VIMDE-Cl was stirred with an excess amount of sodium trifluoroacetate in DMF (20 mL) at 25 °C for 24 h. VIMDE-TFA was obtained after filtration and washing with water and then kept at 60 °C in an oven under reduced pressure for evaporating solvents to get a constant weight.

For preparing MNPs, in a three-neck bottom flask supplied with a magnetic stirrer, connected to a nitrogen inlet, thermometer, and condenser, a mixture of $FeCl_3 \cdot 6H_2O$ (8 g, 29.60 mmol) and $FeCl_2 \cdot 6H_2O$ (2.94 g, 14.80 mmol) was dissolved in deionized water (100 mL). Nitrogen was run with stirring for one h to avoid unwanted Fe^{2+} oxidation. Under N_2 atmosphere, the mixture was stirred and heated at 70 °C for 5 h while adding NH_4OH solution (28%, 20 mL) dropwise. After cooling to 25 °C, MNPs were collected using an external magnet and washed with deionized water. Following this, MNPs (4 g) were dispersed in VIMDE-Cl or VIMDE-TFA solution (2 g of either VIMDE-Cl or VIMDE-TFA dispersed in 50 mL of DMF) and heated at 65 °C for 4 hours under ultra-sonication. The yielded SMNPs were collected with an external magnet and washed with ethanol to remove the VIMDE-Cl and VIMDE-TFA residuals. SMNPs were then dried at 50 °C to constant weight. The obtained SMNPs using VIMDE-Cl and VIMDE-TFA were assigned as VDCL/MNPs and VDTA/MNPs, respectively.

2.2. Compatibility of VDCL/MNPs and VDTA/MNPs with crude oil components

VDCL/MNPs and VDTA/MNPs compatibility with crude oil can be investigated using contact angle measurements. A thin film of VDCL/MNPs and VDTA/MNPs was created on the glass surface, followed by measuring the contact angles of water and crude oil droplets on SMNPs surfaces. Briefly, VDCL/MNPs or VDTA/MNPs (0.5 g) were dispersed in chloroform (3 mL). The dispersed MNPs were spread over the glass slide, followed by chloroform evaporation. A thin film of MNPs on the glass slide was formed by repeating this step several times. A drop-shape analyzer was used for measuring water and oil droplet contact angles on these surfaces.

2.3. Characterization

The formation of cross-linked poly ionic liquids, CPIL, VIMDE-Cl, and VIMDE-TFA, was confirmed with Fourier transform infrared (FTIR) spectroscopy. X-ray diffraction (XRD) was also

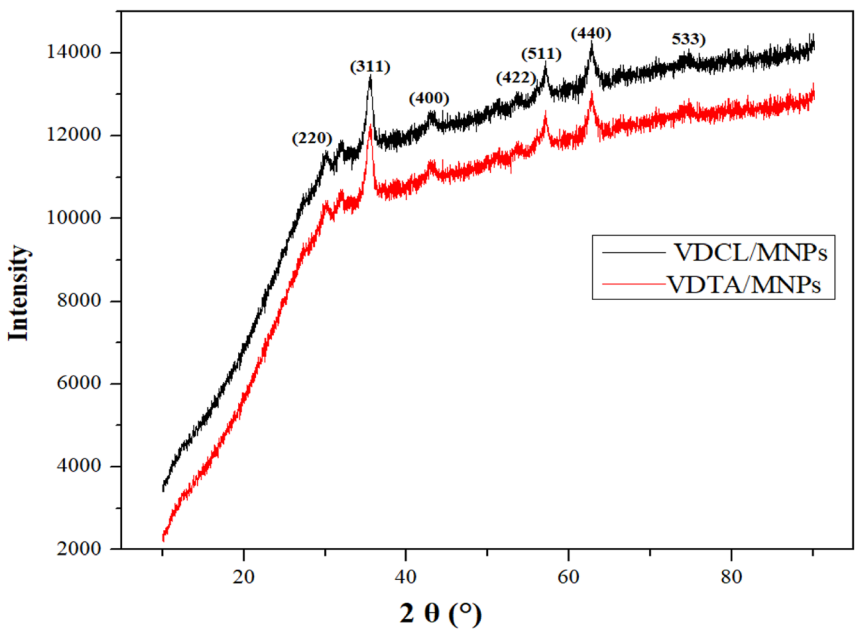

Fig. 2 XRD of VDCL/MNP and VDTA/MNPs.

used to verify VDCL/MNP and VDTA/MNP structures. Thermogravimetric analysis (TGA) was used to study VDCL/MNPs and VDTA/MNPs' thermal stability. Transmission electron microscopy (TEM) and dynamic light scattering (DLS) were employed for determining the particle sizes (PS) and polydispersity index (PDI) of VDCL/MNPs and VDTA/MNPs. VDCL/MNPs and VDTA/MNPs magnetic properties were evaluated by a vibrating sample magnetometer (VSM).

2.4. Evaluation of MNPs' performance in oil spill recovery

MNPs' performance for oil spill recovery was evaluated as reported in our earlier work. Briefly, a crude oil sample (0.2 g) was injected onto the water surface (70 mL) in a 100 mL beaker. Different weight ratios of MNPs were spread over crude oil and left to interact with crude oil components for different periods of time. Following that, MNPs interacting with crude oil were recovered by an external magnet covered with aluminum foil with a known mass. The collected MNPs with recovered crude oil were frozen and lyophilized for 24 h for water removal, followed by their weighing to evaluate the weight of recovered crude oil. The performance of MNPs for oil recovery (PMOR%) was calculated using the following formula:

$$\mathrm{PMOR\%} = \frac{\mathrm{MRO}}{\mathrm{MUO}} \times 100 \quad (1)$$

where MRO is the mass of recovered oil and MUO is the mass of used oil. The residual oil in the water was extracted with chloroform through a separatory funnel to verify the results. After that, chloroform was evaporated using a rotary evaporator, and the residual mass was taken to calculate PMOR.

3 Results and discussions

3.1. Characterization

FTIR spectra confirmed the VIMDE-Cl and VIMDE-TFA chemical structures. Fig. 1(a) and (b) shows the FTIR spectra of VIMDE-Cl and VIMDE-TFA. Due to their similar chemical structure, the spectra for both seem similar. Fig. 1(a) and (b) depicts the disappearance of bending vibration bands of C–H in C=C–H at 962 cm^{-1} and 937 cm^{-1}.[19] In addition, the disappearance of the vibration absorption band of C=C indicated the occurrence of polymerization reactions. The terephthalate carbonyl group vibration band appeared at 1721 cm^{-1}. In the VIMDE-TFA spectrum (Fig. 1b), an additional vibration band appeared at 1680 cm^{-1}, corresponding to the carbonyl group of trifluoroacetate, indicating that the ion exchange of chloride

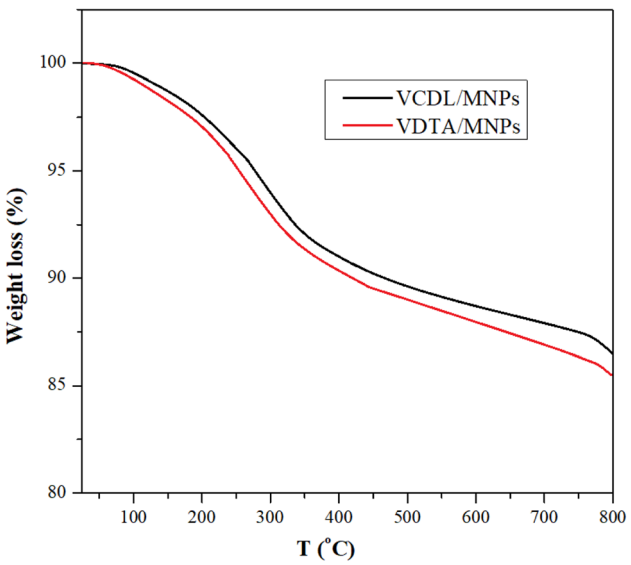

Fig. 3 TGA of VCDL/MNPs and VCTA/MNPs.

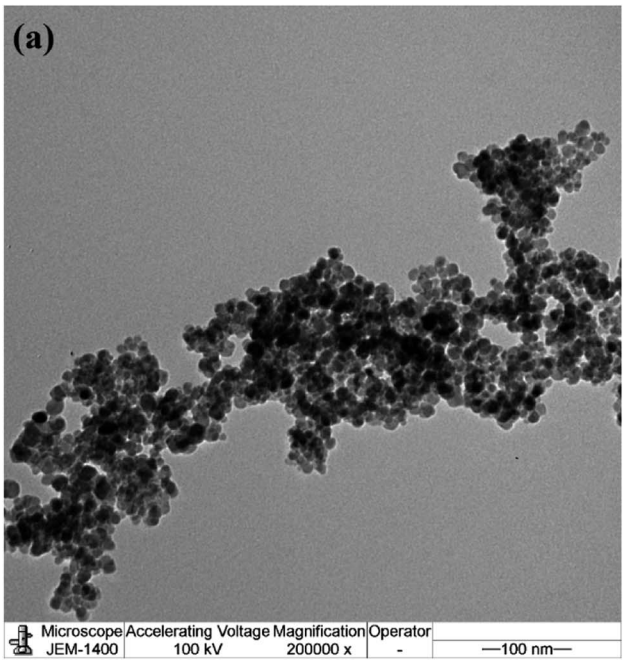

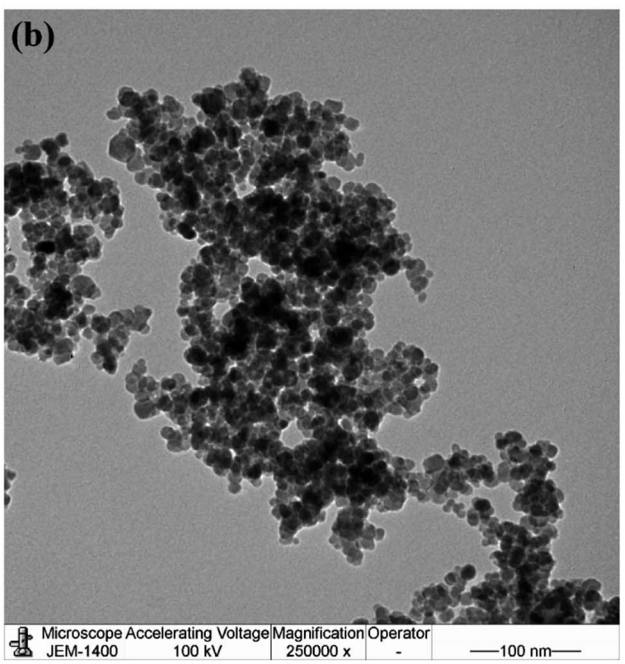

Fig. 4 TEM of (a) VDCL/MNPs and (b) VDTA/MNPs.

with trifluoroacetate occurs.[20] The vibration bands of saturated C–H were noticed at 2926 cm^{-1} and 2856 cm^{-1}. The stretching vibration bands of aromatic C–H in phenyl and imidazolium rings were observed at 3081 cm^{-1} and 3130 cm^{-1}.[21] FTIR technique was also used to verify MNPs surface modification of using VIMDE-Cl, and VIMDE-TFA, as shown in Fig. 1(c) and (d).

VDCL/MNP and VDTA/MNPs FTIR spectra show the same functional groups, suggesting that MNPs have been modified with these materials. Two new extensive bands were found at 626 cm^{-1} and 581 cm^{-1} (ref. 22) connected to FeO-confirmed MNPs formation. VDCL/MNPs and VIMDE-TFA chemical structures were also elucidated by XRD analysis, as illustrated in Fig. 2. The figure shows several characteristic peaks of SMNPs. These peaks appeared at $2\theta = 30.1°$, 35.5°, 43.0°, 53.4°, 57.2°, 62.6°, and 74.4 attributed to the (220), (311), (400), (422), (511), (440), and (533) Miller indexes. The peak at $2\theta = 32.8°$ affirmed MNPs surface modification with VIMDE-Cl and VIMDE-TEA.[23]

The TGA thermograms of VDCL/MNPs and VDTA/MNPs are shown in Fig. 3. The figure depicts the thermal stability of VDCL/MNPs and VDTA/MNPs between 25–800 °C. Weight loss

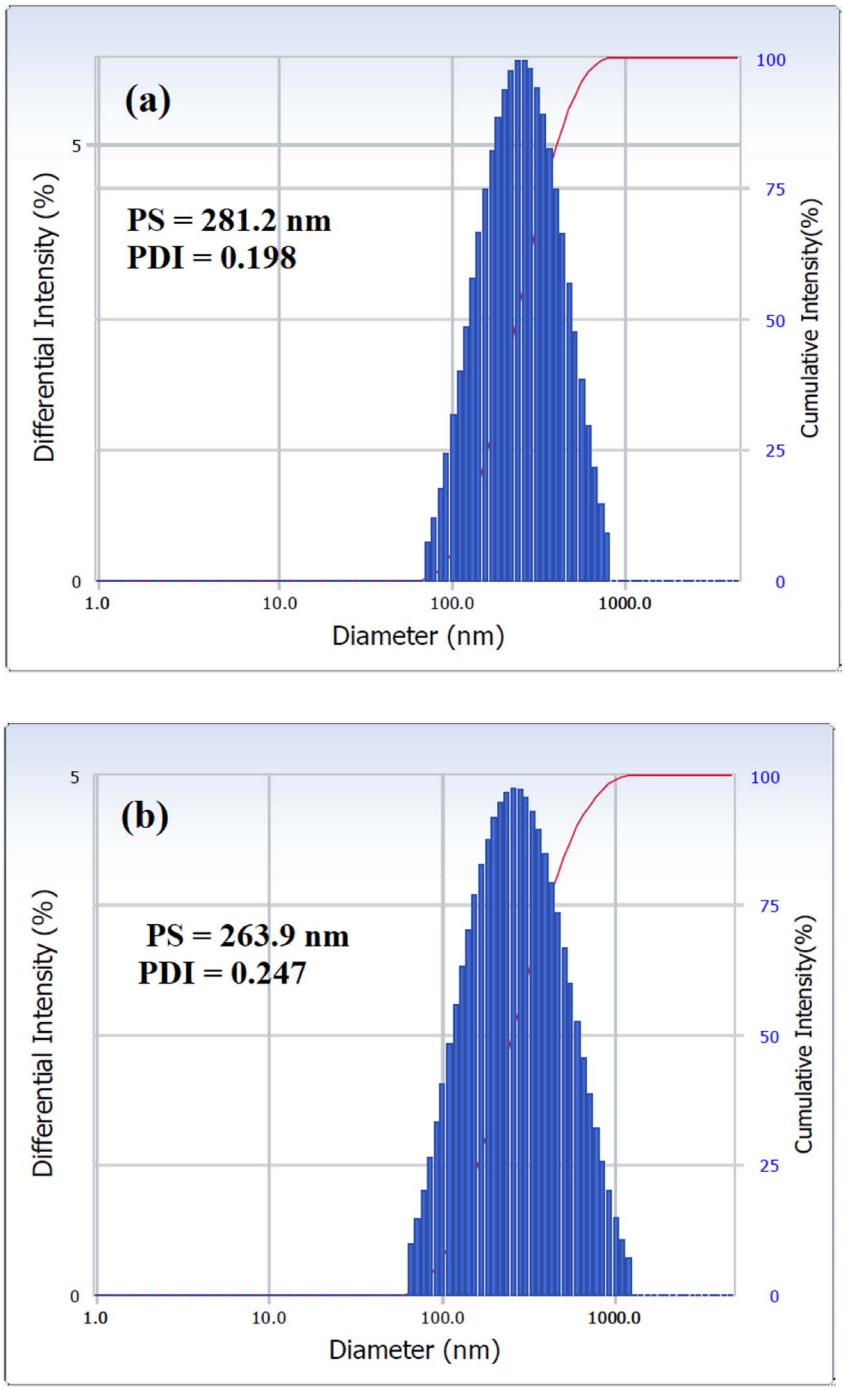

Fig. 5 DLS of (a) VDCL/MNPs and (b) VDTA/MNPs.

up to 150 is 1.5% and 1.8% for VDCL/MNPs and VDTA/MNPs, respectively. Weight loss in this region is likely due to loss of physisorbed water.[24] The weight loss between 150–350 °C is 6.3% and 6.9% for VDCL/MNPs and VDTA/MNPs, respectively, which could be linked to organic constituents' decomposition on MNPs' surface. The weight loss after 350 might result from Fe_2O_3 transformation to FeO with the reduction of iron(III) to iron(II) with carbonaceous residual mass.[25]

The nanosize structure of the prepared SMNPs was confirmed using TEM analysis, as illustrated in Fig. 4(a) and (b). The figure depicts MNPs formation in nanosized structures with an average diameter of 8.2 nm. Additionally, MNPs appeared in cluster form, likely due to their magnetic nature as they attract each other, forming clusters.[26] PS and PDI of VCDL/MNPs and VCTA/MNPs in chloroform were measured using the DLS technique, as depicted in Fig. 5(a) and (b). PS and PDI are 281.2 nm and 0.198, respectively, for VCDL/MNPs, while they are 263.9 nm and 0.247, respectively, for VCTA/MNPs. The difference between PS measured with TEM and DLS could be linked to VCDL/MNPs and VCTA/MNPs behavior in chloroform due to their interaction, forming clusters.[27]

VDCL/MNPs and VDTA/MNPs compatibility with crude oil components was examined by measuring the contact angles of water and crude oil droplets on their surfaces, as mentioned in the Experimental section. Droplets of crude oil spread on the surfaces of VDCL/MNPs and VDTA/MNPs, giving a 0° value reflecting the compatibility between crude oil and SMNPs. Fig. 6(a) and (b) shows the contact angle of water droplets on VDCL/MNPs and VDTA/MNPs surfaces. Water droplet contact angles are 100.8° and 111.4° for VDCL/MNPs and VDTA/MNPs, respectively. The contact angle values suggested the hydrophobicity of SMNPs and their ability to interact with and disperse in oil more than water. In addition, a water droplet on VDTA/MNPs surface exhibited a higher contact angle than VDCL/MNPs, possibly due to using VIMDE-TFA for MNPs surface modification in VDTA/MNPs, as IMDE-TFA has a trifluoroacetate group in its structure.[20]

The magnetic properties of MNPs are a crucial parameter for their application in oil spill recovery, as they can be collected easily using an external magnetic field. Herein, the magnetic properties of VDCL/MNPs and VDTA/MNPs, including saturation magnetization (M_s), magnetic remanence (M_r), and coercivity (H_c), were measured with VSM, as illustrated in Table 1. M_s values indicate that VDCL/MNPs and VDTA/MNPs respond effectively to external magnetic fields. The low M_r and H_c values indicated the absence of coercivity and remanence at room temperature. The results also exhibited a higher M_s value of VDTA/MNPs than that of VDTA/MNPs, which may be due to decreased VIMDE-Cl on MNPs' surface than VDTA/MNPs; these data are compatible with TGA results.

3.2. Application of MNPs for oil spill recovery

TEM and DLS measurements confirmed the nano-size structures of VDCL/MNPs and VDTA/MNPs. CA and VSM measurements also confirmed their compatibility with oil components and the ease of collecting them using an external magnet. These

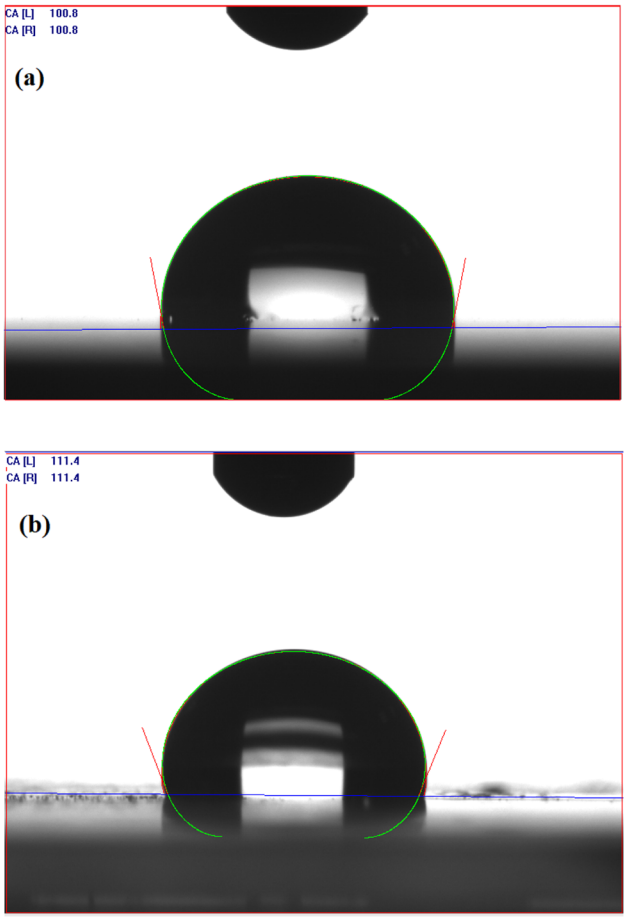

Fig. 6 Contract angles of water droplet on (a) VDCL/MNPs and (b) VDTA/MNPs.

Table 1 Magnetic properties of VDCL/MNPs and VDTA/MNPs at 25 °C

SMNPs	M_s (emu g^{-1})	M_r (emu g^{-1})	H_c (Oe)
VDCL/MNPs	54	0.081	3.2
VDTA/MNPs	61	0.094	4.6

properties recommend using these MNPs for oil spill recovery. For that, the performance of MNPs for oil spill recovery (PMOR) was evaluated using different weights of crude oil : water. The contact time effect on PMOR was also evaluated.

3.2.1. Contact time effect. Contact time significantly affects PMOR, as MNPs need time to interact with oil components. The contact time effect on PMOR was evaluated using a crude oil : water ratio of 1 : 4, as shown in Fig. 7. As depicted in the figure, the PMOR rises with time, reaching a maximum of 6 min. In the beginning, PMOR increased significantly, likely due to the large number of vacant sites on VDCL/MNPs and VDTA/MNPs surfaces.[28] After that, PMOR increased slightly with time as most of these sites became occupied by adsorbed crude oil, reaching maximum values of 89% and 97%, respectively, for VDCL/MNPs and VDTA/MNPs at 6 min. When these results were compared with previous studies that used ILs for MNPs surface

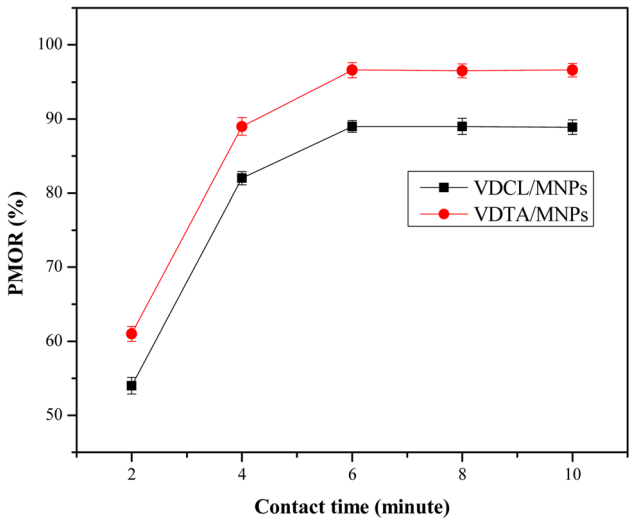

Fig. 7 PMOR of VDCL/MNPs and VDTA/MNPs against contact time.

modification,[25,27] VDCL/MNPs and VDTA/MNPs reached equilibrium in a shorter contact time, possibly due to variation of groups in IL structure, as they contain aromatic, aliphatic, and heteroatoms, making them more compatible with crude oil components.

3.2.2. MNPs : crude oil ratio effect. The effect of MNPs : crude oil ratios was also evaluated using different weight ratios (1 : 1, 1 : 2, 1 : 4, 1 : 10, 1 : 15, 1 : 20, and 1 : 25). Fig. 8 depicts the relation between PMOR of VDCL/MNPs and VDTA/MNPs and MNPs : crude oil ratio. The data exhibited an increase in PMOR with increased MNPs ratio, reaching maximum values of 99% and 96% for VDCL/MNPs and VDTA/MNPs, respectively, at MNPs : crude oil ratio of 1 : 1. Fig. 9 shows optical photos of oil spilled over the water surface, dispersed SMNPs on the oil surface, and collected SMNPs and oil on their surfaces after 6 minutes at a SMNPs : crude oil ratio of 1 : 2 using. As shown in

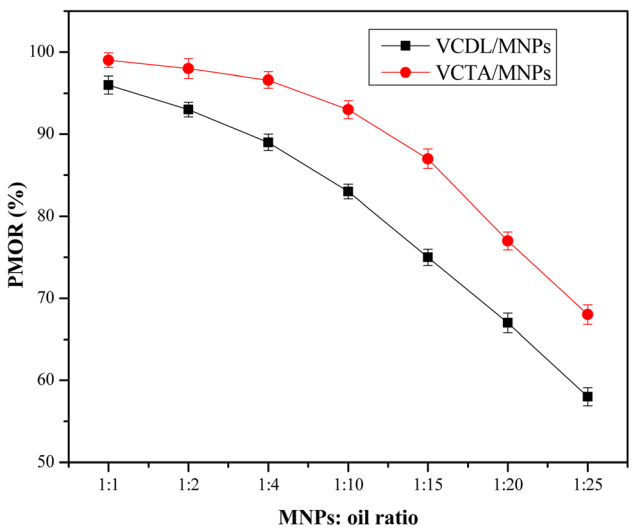

Fig. 8 PMOR of VDCL/MNPs and VDTA/MNPs against MNPs : crude oil ratio.

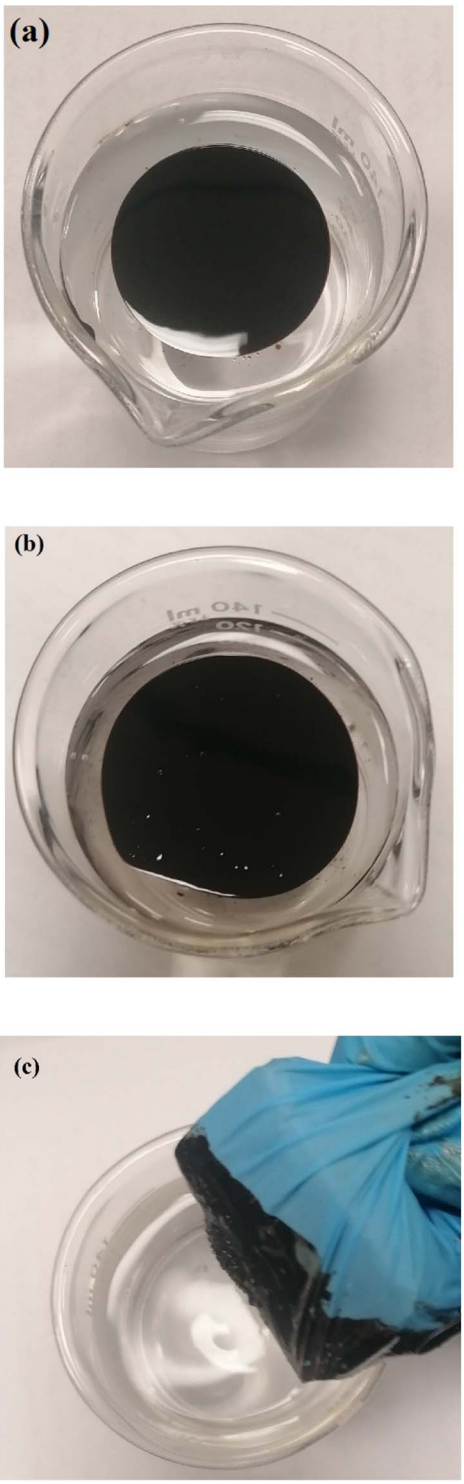

Fig. 9 Optical photos of (a) oil spill over water surface, (b) dispersed SMNPs over oil surface, and (c) collected SMNPs and oil on their surfaces.

Fig. 9(b), VDTA/MNPs go through crude oil, indicating the interaction between SMNPs and oil components as SMNPs do not stay over the oil surface or settle down in the bottom of the beaker. After the adsorption of SMNPs with adsorbed oil on the external magnet, the water surface appears clean (Fig. 9(c)).

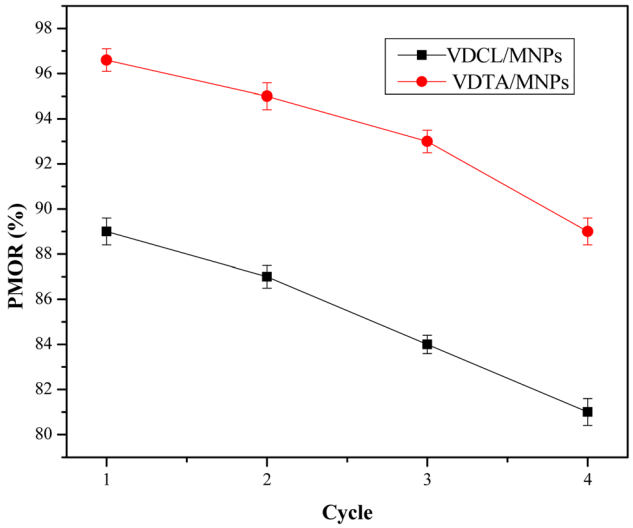

Fig. 10 PMOR of VDCL/MNPs and VDTA/MNPs against reusability cycles.

3.2.3. Reusability of VDCL/MNPs and VDTA/MNPs. The reusability of SMNPs, VDCL/MNPs, and VDTA/MNPs was evaluated in four cycles. To do so, the used MNPs were washed with chloroform, then acetone, and finally dried at 25 °C. The reused MNPs were utilized for the next cycle. Fig. 10 represents SMNP reusability in four cycles. The figure shows that VDCL/MNPs and VDTA/MNPs exhibited significant PMOR in these four cycles. However, PMOR decreases with cycle number increase. As the cycle progressed from the first to the fourth, the PMOR of VDCL/MNPs declined from 89% to 81%. In contrast, PMOR decreased from 96.6% to 89% for VDTA/MNPs. Such decrease may be due to a change in SMNPs hydrophobicity.[29]

4 Conclusion

PET waste was used for synthesizing two new CPILs, VIMDE-Cl and VIMDE-TFA. The produced CPILs, VIMDE-Cl and VIMDE-TFA, were utilized for MNPs surface modification, yielding SMNPs, VDCL/MNPs, and VDTA/MNPs, respectively. The structures of CPILs, VIMDE-Cl and VIMDE-TFA, and SMNPs, VDCL/MNPs, and VDTA/MNPs were confirmed with FTIR and XRD. Additionally, the PS and magnetic properties of VDCL/MNPs and VDTA/MNPs were measured using TEM, DLS, and VSM techniques. VDCL/MNPs and VDTA/MNPs compatibility with oil components was evaluated using contact angle measurements.

Contact angle and VSM measurements suggested SMNP compatibility with oil components and the ease of collecting them using an external magnet. Accordingly, they can be applied to oil spill recovery in marine environments. The PMOR of VDCL/MNPs and VDTA/MNPs was evaluated using different MNPs : crude oil ratio (ranging from 1 : 1 to 1 : 25). The contact time effect on PMOR was also evaluated. VDCL/MNPs and VDTA/MNPs exhibited significant PMOR with an increasing SMNPs ratio. PMOR reached maximum values of 99% and 96% for VDCL/MNPs and VDTA/MNPs, respectively, at SMNPs : crude oil ratio of 1 : 1. Furthermore, the data exhibited that the optimal contact time for obtaining the highest PMOR is 6 min for both where the PMOR reached maximum values of 89% and 97%, respectively for VDCL/MNPs and VDTA/MNPs at SMNPs : crude oil ratio of 1 : 4. Finally, the accumulative results indicated how solid waste can be used as a precursor for preparing effective SMNPs and applying them for oil spill recovery, solving two environmental issues, solid waste reduction, and oil spill remediation.

Conflicts of interest

There are no conflicts to declare.

Acknowledgements

The authors acknowledge the financial support through Researchers Supporting Project number (RSP2023R54), King Saud University, Riyadh, Saudi Arabia.

References

1 R. Hamade, R. Hadchiti and A. Ammouri, Making the environmental case for reusable PET bottles, *Procedia Manuf.*, 2020, **43**, 201–207.
2 A. M. Atta, W. Brostow, T. Datashvili, R. A. El-Ghazawy, H. E. H. Lobland, A. R. M. Hasan and J. M. Perez, Porous polyurethane foams based on recycled poly (ethylene terephthalate) for oil sorption, *Polym. Int.*, 2013, **62**(1), 116–126.
3 A. M. Atta, M. E. Abdel-Rauf, N. E. Maysour, A. Abdul-Rahiem and A.-A. A. Abdel-Azim, Surfactants from recycled poly (ethylene terephthalate) waste as water based oil spill dispersants, *J. Polym. Res.*, 2006, **13**, 39–52.
4 A. M. Atta, M. A. Elsockary, O. F. Kandil and N. O. Shaker, Nonionic surfactants from recycled poly (ethylene terephthalate) as corrosion inhibitors of steel in 1 M HCl, *J. Dispersion Sci. Technol.*, 2008, **29**(1), 27–39.
5 R. Abd El-Hameed, Aminolysis of polyethylene terephthalate waste as corrosion inhibitor for carbon steel in HCl corrosive medium, *Adv. Appl. Sci. Res.*, 2011, **2**(3), 483–499.
6 M.-J. Li, Y.-H. Huang, A.-Q. Ju, T.-S. Yu and M.-Q. Ge, Synthesis and characterization of azo dyestuff based on bis (2-hydroxyethyl) terephthalate derived from depolymerized waste poly (ethylene terephthalate) fibers, *Chin. Chem. Lett.*, 2014, **25**(12), 1550–1554.
7 Y. Wang, X. Wang, W. Lu, Q. Yuan, Y. Zheng and B. Yao, A thin film polyethylene terephthalate (PET) electrochemical sensor for detection of glucose in sweat, *Talanta*, 2019, **198**, 86–92.
8 F. Cui, H. Jafarishad, Z. Zhou, J. Chen, J. Shao, Q. Wen, Y. Liu and H. S. Zhou, Batch fabrication of electrochemical sensors on a glycol-modified polyethylene terephthalate-based microfluidic device, *Biosens. Bioelectron.*, 2020, **167**, 112521.
9 M. M. Abdullah and H. A. Al-Lohedan, Demulsification of water in heavy crude oil emulsion using a new amphiphilic

ionic liquid based on the glycolysis of polyethylene terephthalate waste, *J. Mol. Liq.*, 2020, **307**, 112928.

10 M. M. Abdullah, H. A. Al-Lohedan and A. M. Atta, Fabrication of new demulsifiers employing the waste polyethylene terephthalate and their demulsification efficiency for heavy crude oil emulsions, *Molecules*, 2021, **26**(3), 589.

11 M. M. Abdullah and H. A. Al-Lohedan, Novel amphiphilic gemini ionic liquids based on consumed polyethylene terephthalate as demulsifiers for Arabian heavy crude oil, *Fuel*, 2020, **266**, 117057.

12 H. Singh, N. Bhardwaj, S. K. Arya and M. Khatri, Environmental impacts of oil spills and their remediation by magnetic nanomaterials, *Environ. Nanotechnol., Monit. Manage.*, 2020, **14**, 100305.

13 M. Chen, W. Jiang, F. Wang, P. Shen, P. Ma, J. Gu, J. Mao and F. Li, Synthesis of highly hydrophobic floating magnetic polymer nanocomposites for the removal of oils from water surface, *Appl. Surf. Sci.*, 2013, **286**, 249–256.

14 A. M. Pintor, V. J. Vilar, C. M. Botelho and R. A. Boaventura, Oil and grease removal from wastewaters: sorption treatment as an alternative to state-of-the-art technologies. A critical review, *Chem. Eng. J.*, 2016, **297**, 229–255.

15 D. Dave and A. E. Ghaly, Remediation technologies for marine oil spills: a critical review and comparative analysis, *Am. J. Environ. Sci.*, 2011, **7**(5), 423.

16 Y. Mahajan, Nanotechnology-based solutions for oil spills, *Nat. Nanotechnol.*, 2011, **2**(1), 1–19.

17 B. Singh, S. Kumar, B. Kishore and T. N. Narayanan, Magnetic scaffolds in oil spill applications, *Environ. Sci.: Water Res. Technol.*, 2020, **6**(3), 436–463.

18 M. M. Abdullah and H. A. Al-Lohedan, Alginate-based poly ionic liquids for the efficient demulsification of water in heavy crude oil emulsions, *Fuel*, 2022, **320**, 123949.

19 X.-F. Wang, Y. Zhang, Y. Shu, X.-W. Chen and J.-H. Wang, Ionic liquid poly (3-n-dodecyl-1-vinylimidazolium) bromide as an adsorbent for the sorption of hemoglobin, *RSC Adv.*, 2015, **5**(40), 31496–31501.

20 M. M. Abdullah and H. A. Al-Lohedan, Demulsification of Arabian Heavy Crude Oil Emulsions Using Novel Amphiphilic Ionic Liquids Based on Glycidyl 4-Nonylphenyl Ether, *Energy Fuels*, 2019, **33**(12), 12916–12923.

21 T. Rajkumar and G. R. Rao, Synthesis and characterization of hybrid molecular material prepared by ionic liquid and silicotungstic acid, *Mater. Chem. Phys.*, 2008, **112**(3), 853–857.

22 M. I. Khalil, Co-precipitation in aqueous solution synthesis of magnetite nanoparticles using iron (III) salts as precursors, *Arabian J. Chem.*, 2015, **8**(2), 279–284.

23 S. Melhi, M. Algamdi, A. A. Alqadami, M. A. Khan and E. H. Alosaimi, Fabrication of magnetically recyclable nanocomposite as an effective adsorbent for the removal of malachite green from water, *Chem. Eng. Res. Des.*, 2022, **177**, 843–854.

24 Z. Durmus, H. Kavas, M. S. Toprak, A. Baykal, T. G. Altınçekiç, A. Aslan, A. Bozkurt and S. Coşgun, L-lysine coated iron oxide nanoparticles: synthesis, structural and conductivity characterization, *J. Alloys Compd.*, 2009, **484**(1–2), 371–376.

25 M. Abdullah, M. S. Ali and H. A. Al-Lohedan, Oil Spill Cleanup Employing Surface Modified Magnetite Nanoparticles Using Two New Polyamines, *J. Chem.*, 2023, **2023**, 7515345.

26 C. Schweiger, C. Pietzonka, J. Heverhagen and T. Kissel, Novel magnetic iron oxide nanoparticles coated with poly (ethylene imine)-g-poly (ethylene glycol) for potential biomedical application: synthesis, stability, cytotoxicity and MR imaging, *Int. J. Pharm.*, 2011, **408**(1–2), 130–137.

27 M. M. Abdullah, N. A. Faqihi, H. A. Al-Lohedan, Z. M. Almarhoon and F. Mohammad, Fabrication of magnetite nanomaterials employing novel ionic liquids for efficient oil spill cleanup, *J. Environ. Manage.*, 2022, **316**, 115194.

28 E. M. Soliman, S. A. Ahmed and A. A. Fadl, Adsorptive removal of oil spill from sea water surface using magnetic wood sawdust as a novel nano-composite synthesized via microwave approach, *J. Environ. Health Sci. Eng.*, 2020, **18**, 79–90.

29 M. M. Abdullah and H. A. Al-Lohedan, Fabrication of environmental-friendly magnetite nanoparticle surface coatings for the efficient collection of oil spill, *Nanomaterials*, 2021, **11**(11), 3081.